Beyond Monte Carlo: A Computational Framework for Uncertainty Propagation in Planetary Entry, Descent and Landing

Abhishek Halder* and Raktim Bhattacharya†
Texas A&M University, College Station, Texas 77843-3141

Space system verification and validation require high fidelity simulations to predict system performance in presence of uncertainties in the spacecraft and environment. Brute-force Monte Carlo (MC) simulations are overly resource-expensive for such high-dimensional nonlinear systems. A computational framework for uncertainty propagation in planetary entry, descent and landing is proposed that goes beyond traditional MC based dispersion analysis. The methodology and simulation results for this transfer operator based method are provided and compared with MC results to bring forth the computational efficacies.

Nomenclature

h	Altitude
ζ	Latitude
λ	Longitude
V	Mars-relative velocity
γ	Flight path angle
χ	Velocity azimuth angle measured from North
σ	Bank angle
ρ	Martian atmospheric density
ρ_0	Reference-level density
B_c	Ballistic coefficient
$\frac{C_L}{C_D}$	Lift-to-drag ratio
R_0	Mean equatorial radius of Mars
g	Acceleration due to gravity $\approx \frac{GM}{(R_0+h)^2}$, where GM is the Gravitational constant for Mars
Ω	Rotational angular velocity for Mars
v_c	Normalizing velocity constant $= \sqrt{\frac{\mu}{R_0}}$, where $\mu = gR_0^2$
$\mathbf{x}$	State vector
$\mathbf{p}$	Parameter vector
$\mathbf{f}$	Dynamics vector
$\mathbf{X}$	Augmented state vector
$\mathbf{F}$	Augmented dynamics vector
n_s	Number of states
n_p	Number of parameters
t	Time
φ	Probability density function
Ψ	Trace of the Jacobian of the dynamics
Subscript	
i	Variable number

*Graduate Student, Department of Aerospace Engineering, 3141 TAMU, Member AIAA, ahalder@tamu.edu
†Assistant Professor, Department of Aerospace Engineering, 3141 TAMU, Member AIAA, raktim@tamu.edu

I. Introduction

The hypersonic flight during critical mission phases such as planetary entry, descent and landing (EDL) is considered to be one of the most challenging flight regimes for mission design and analysis. Lack of high fidelity modeling, navigational errors are few among many factors which greatly contribute to the off-nomial trajectories during actual mission. Thus assesment of risk and incorporating that knowledge for the purpose of robust mission design supported by statistical verification and validation becomes inevitable. More precisely, one must account for the associated uncertainties in both the initial conditions and in the system parameters such that a probabilistic quantification can be obtained for being inside or outside some pre-defined operational safety margin for all possible off-design trajectories resulted due to the uncertainties.

From simulation point of view, the above becomes a challenging task as ideally one would require to simulate infinite such trajectories for some given bounded uncertainties in the states and parameters of the governing dynamics. Traditionally, a Monte Carlo (MC) dispersion analysis is done for this purpose where one simulates a large number of trajectories for randomly sampled initial conditions and parameter values. If most or all of such trajectories remain inside the safety margin, one can at best hope for the system safety and reliability without any quantitative guarantee whatsoever. Usually the engineers responsible for subsystem models identify the uncertainty bounds and decide about the sampling strategy based on their experience. Clearly, brute force MC simulations are not the best approach for such mission critical uncertainty analysis. Moreover, for high dimensional and nonlinear dynamics like spacecraft EDL, MC simulations are tremendously expensive as one strives to simulate individual trajectories one by one for uncertainties in hundreds of states and parameters and their combinations. In spite of all these drawbacks, almost all space mission uncertainty analysis are done with MC simulations including Mars Pathfinder,[1] METEOR[2] recovery module, Stardust[3] comet sample return capsule, Mars Microprobe,[4] Mars Surveyor Program 2001 Orbiter and Lander[5] and to-be-launched Mars Science Laboratory[6] (MSL) mission. In fact, many important decisions in mission design have been historically driven by MC based dispersion analysis. Mars landing site selection, design of the Pathfinder aeroshell thermal protection system[7] and parachute deployment algorithm[1] are examples for the same. This heavy bias towards MC simulations among EDL analysis practitioners is partly due to its ease of implementation and partly due to the scarcity of alternative analysis methods.

An alternative to simulating trajectory is to simulate the evolution of density. In other words, instead of studying individually sampled random initial condition with random parameter values, one can study how a given distribution of initial conditions and parameters evolve over time. The successive probability densities are given by a linear integral operator, known as the Perron-Frobenius (PF) operator. The PF operator essentially governs the spatio-temporal evolution of the probability density function (pdf) subject to the (in general nonlinear) system dynamics. A thorough treatment of PF operator based density evolution can be found in Lasota and Mackey.[8] Counter-intuitive examples are given in the same reference showing finite number of trajectory simulations can yield misleading result depending on the system dynamics, whereas PF operator based method serves as a unified framework which allows density evolution subject to any dynamics, both deterministic and stochastic, both continuous and discrete, and is naturally suitable for uncertainty analysis in the non-parametric sense (in terms of the pdf). All statistical moments can be retrieved from the pdf.

Our primary objective in this paper is to demonstrate a PF operator based method for uncertainty analysis for the EDL problem which we deem to be superior than MC approach. We will use the transport equation associated with the PF operator that convects the probability mass as the system evolves with the underlying dynamics. It can be shown that[8] for the case of deteministic dynamics, this transport equation reduces to the Liouville equation,[9] which is a linear partial differential equation (PDE). For simplicity, we will restrict ourselves to deterministic dynamics only. Our purpose is to show that the PDE can be easily solved numerically using the method of characteristics and thus one can obtain exact pdfs with significant computational savings as opposed to crudely approximating the pdfs through traditional large-scale MC simulations. The key point here is the scalability of the PF operator based approach compared to MC simulations, which suffer from the 'curse of dimensionality'. This is why, we argue that, PF operator is naturally suited for uncertainty analysis in high-dimensional nonlinear systems like planetary EDL.

II. Nonlinear Flight Dynamics

We will work with Vinh's equations[10] for hypersonic EDL. We will start with the simpler three state model assuming the dynamics to be purely longitudinal and then describe the more general six-state model. These equations govern the trajectory of the center-of-mass of the spacecraft entering into the Mars atmosphere.

A. Three state model

For the simplified case that the entire trajectory is contained in the longitudinal plane, we get the following three state (h, V, γ) model for non-rotating spherical Mars with zero bank angle flight.

$$\dot{h} = V \sin\gamma \tag{1a}$$

$$\dot{V} = -\frac{\rho R_0}{2B_c} V^2 - \frac{gR_0}{v_c^2} \sin\gamma \tag{1b}$$

$$\dot{\gamma} = \frac{\rho R_0}{2B_c} \frac{C_L}{C_D} V + \frac{gR_0}{v_c^2} \cos\gamma \left(\frac{V}{R_0 + h} - \frac{1}{V} \right) \tag{1c}$$

Here the model for Martian atmospheric density variation[11] is taken as

$$\rho = \rho_0 \exp\left(\frac{h_2 - hR_0}{h_1} \right) \tag{2}$$

where $h_2 = 20$ km and $h_1 = 9.8$ km. The mean equatorial radius of Mars will be taken as $R_0 = 3397$ km.

B. Six state model

Here we present the more general form of Vinh's equations, which is a six state $(h, \theta, \phi, V, \gamma, \psi)$ model. This model takes the self-rotation of the planet and the bank angle (σ) into account.

$$\dot{h} = V \sin\gamma \tag{3a}$$

$$\dot{\theta} = \frac{V \cos\gamma \cos\psi}{(R_0 + h)\cos\phi} \tag{3b}$$

$$\dot{\phi} = \frac{V \cos\gamma \sin\psi}{(R_0 + h)} \tag{3c}$$

$$\dot{V} = -\frac{\rho R_0}{2B_c} V^2 - \frac{gR_0}{v_c^2} \sin\gamma + \Omega^2 (R_0 + h) \cos\phi (\sin\gamma \cos\phi - \cos\gamma \sin\phi \sin\psi) \tag{3d}$$

$$\dot{\gamma} = \frac{\rho R_0}{2B_c} \frac{C_L}{C_D} V \cos\sigma + \frac{gR_0}{v_c^2} \cos\gamma \left(\frac{V}{R_0 + h} - \frac{1}{V} \right) \tag{3e}$$

$$\dot{\psi} = \frac{\rho R_0}{2B_c} \frac{C_L}{C_D} \frac{V \sin\sigma}{\cos\gamma} - \frac{V \cos\gamma}{(R_0 + h)} \tan\phi \cos\psi + 2\Omega (\tan\gamma \cos\phi \sin\psi - \sin\phi) - \frac{\Omega^2 (R_0 + h)}{V \cos\gamma} \sin\phi \cos\phi \cos\psi \tag{3f}$$

Ω was calculated from the rotational time period of Mars, which is 24 hours 39 minutes and 35.24 seconds. The density variation is taken identical to the three-state model.

III. Uncertainty modeling

In this paper, we will deal with uncertainty in the probabilistic sense (this is sometimes called *aleatoric uncertainty* as opposed to the structured or *epistemic uncertainty*). In general, we will assume uncertainty in the states $\mathbf{x} = [h\ \theta\ \phi\ V\ \gamma\ \psi]^T$ and in the parameters $\mathbf{p} = \left[\rho_0\ B_c\ \frac{C_L}{C_D}\right]^T$. The state model as described in Section II is of the form

$$\dot{\mathbf{x}} = \mathbf{f}(\mathbf{x}, \mathbf{p}), \quad \mathbf{x} \in \mathbb{R}^{n_s},\ \mathbf{p} \in \mathbb{R}^{n_p} \tag{4}$$

which can be put in an augmented form

$$\dot{\mathbf{X}} = \mathbf{F}(\mathbf{X}), \quad \mathbf{X} \in \mathbb{R}^{n_s + n_p} \tag{5}$$

where $\mathbf{X} = [\mathbf{x}\ \mathbf{p}]^T$ is the augmented state vector.

The transport of the probabilistic uncertainty subject to the deterministic dynamics (Eqn. (5)) is governed by the Liouville equation

$$\frac{\partial \varphi(\mathbf{X},t)}{\partial t} + \sum_{i=1}^{n_s} \frac{\partial}{\partial X_i}\left[\varphi(\mathbf{X},t)\, F_i(\mathbf{X})\right] = 0 \tag{6}$$

which is a linear PDE associated with the PF operator. Here $\varphi(\mathbf{X},t)$ is the joint pdf. Along the trajectory, one can reduce (cf. Mellodge and Kachroo,[12] §8.1.2) the above PDE to an ordinary differential equation (ODE) of the form

$$\frac{d\varphi(\mathbf{X},t)}{dt} = -\varphi(\mathbf{X},t)\,\Psi(\mathbf{X}) \tag{7}$$

where $\Psi(\mathbf{X}) = \sum_{i=1}^{n_s} \frac{\partial F_i}{\partial X_i}$ is the trace of the Jacobian of the underlying dynamics and hence, evolves with time. At this point, it's apparent that if the intial state and parametric uncertainties are specified in terms of a joint pdf $\varphi_0 := \varphi(\mathbf{X}(0),0)$, then one can write the solution of Eqn. (7) as

$$\varphi(\mathbf{X},t) = \varphi_0 \exp\left(-\int_0^t \Psi(\mathbf{X}(\tau))\, d\tau\right). \tag{8}$$

In general, it's hardly possible to evaluate the integral in Eqn. (8) analytically and thus mandates numerical solution. Once the solution for the joint pdf $\varphi(\mathbf{X},t)$ is obtained, one can find the marginal pdfs by integrating out the other states over their respective domains, namely

$$\varphi(X_i,t) = \int_{\mathcal{D}_1} ... \int_{\mathcal{D}_{i-1}} \int_{\mathcal{D}_{i+1}} ... \int_{\mathcal{D}_{n_s}} \varphi(\mathbf{X},t)\, dX_1 ... dX_{i-1} dX_{i+1} ... dX_{n_s} \tag{9}$$

where $\mathcal{D}_i$ is the domain of the i^{th} state variable at time t. Here it's important to realize that since the domain in the state space is deforming with time, one must know the instantaneous domain to carry out the integration in Eqn. (9). We will talk more about this later.

IV. Numerical Simulations: Methodology and Results

Two kinds of numerical simulations were performed for obtaining the marginal pdfs for the states involved in the Vinh's equation. In the PF operator based approach, initial uncertainties in the states and parameters were transcripted as an initial joint pdf, which was then propagated by the Liouville's equation. On contrary, in the MC approach, a large number of random initial conditions and parameter values were chosen to simulate many trajectories and from there, an approximation of the pdf was obtained by plotting the histograms.

We assumed that both the states and the parameters have 5% uniform uncertainties about their respective nominal values (denoted by tilde). The nominal values of the parameters were taken as $\widetilde{B}_c = 72.8$ kg/m^2, $\widetilde{\rho}_0 = 0.0019$ kg/m^3 and $\frac{\widetilde{C_L}}{\widetilde{C_D}} = 0.3$. The same for the intial conditions were chosen as $\widetilde{h} = 80$ km, $\widetilde{\theta} = 341.03°$E, $\widetilde{\phi} = 24.01°$N, $\widetilde{V} = 3500$ m/sec, $\widetilde{\gamma} = -2°$ and $\widetilde{\psi} = 0°$. We mention here that the nomial latitude-longitude pair corresponds to the Mawrth Vallis,[13] one of the final four candidates[14] for MSL landing site at Mars. Fourth order Runge-Kutta scheme was employed for both the methods with step size of 0.01 (non-dimensional time step). For all results provided here, the integration was carried up to 60 such nondimensional time steps.

In Fig.1, we have shown the 267^{th} second's (physical time) snapshots of marginal pdfs for the three state model with uncertainties in the states only.This simpler case with no parametric uncertainties provides insight into the difficulties associated with the MC method and how they can be tackled in the PF operator approach. It can be observed that a MC simulation with 10 *discretizations per dimension* (henceforth *dpd*) results rather "groovy" histogram approximations of the pdfs (Fig.1). Smoother pdfs can be obtained through PF operator method using the same dpd. Increasing the number of dpd slightly smoothens out the MC histograms (Fig.1(c)-(d)), but only at the expense of computational time. Thus, an effort to obtain good approximation of the pdf using MC method incurs the 'curse of dimensionality' which loosely refers to the

exponential growth in computational time with increasing dpd. This is illustrated in Fig.2. All simulations were done on a 64 bit CPU with 2.8 GHz processor. On contrary, similar or even smoother pdfs can be computed by PF operator method with less samples and the result is exact in the sense that instead of approximating a pdf by histogram bin-counting (as in MC method), one propagates the pdf (probability weight) itself.

At this point, our case study with the three state model has demonstrated how MC is challenged by computational tractability for the sake of accuracy. The problem gets further aggravated if we consider the three state model with both state and parametric uncertainties. Although the parameters don't evolve themselves, uncertainties therein affect the computation since one needs to grid the extended state space (see Eqn. (5)). The six state model exacerbates the situation further. One can get a quantitative idea from Table 1 where we listed the CPU times needed for different cases.

Table 1. Comparison of computational times for different cases for the three and six state model using PF and MC method

Three state model

Method	Only state uncertainties	Both state and parametric uncertainties
PF (dpd = 10)	0.522 sec (3.1 MB)	7 min 00.865 sec (2.6 GB)
MC (dpd = 10)	0.424 sec	6 min 54.279 sec (2.1 GB)
MC (dpd = 30)	11.263 sec	Requires more than 3 days (85 hours approx.)
MC (dpd = 40)	26.936 sec	Not attempted
MC (dpd = 60)	1 min 30.176 sec	Not attempted
MC (dpd = 100)	7 min 02.221 sec	Not attempted

Six state model

Method	Only state uncertainties	Both state and parametric uncertainties
PF (dpd = 10)	17 min 27.819 sec (3.9 GB)	Requires days with more than 4 GB file size
MC (dpd = 10)	13 min 01.188 sec (3.6 GB)	Requires days with more than 4 GB file size

It can be noticed that for a three state model with both state and parametric uncertainties, MC simulations with 30 or more dpd take exorbitant computational time. Similar trends follow for the six state model. Furthermore, even with dpd = 10, the output files are of size more than 2 GB for both PF and MC method. This brings forth another computational challenge, namely post-processing of the huge data. Although handling data of such size is cumbersome for any method, it's more so for the PF operator based approach. Since this method directly propagates the joint pdf, the output file is of the form of a three dimensional array with time being the third dimension. At any fixed time, we have samples as the rows and states and the joint pdf as the columns. While handling moderate filesizes (e.g. Fig. 1(b)), the unstructured non-uniform joint pdf data residing over the instantaneous state space (deforming due to the dynamics), were interpolated on a denser uniform grid after generating connectivity graph using the Delaunay triangulation, on which the integrations in Eqn. (9) were done, one at a time, by employing the trapezoidal rule. However, this strategy is difficult to apply in higher dimensions since the computational burden for this post-processing becomes unsurmountable. Moreover, as Fig. 1 might suggest, the numerical strategy does not yield a very good resolution of the pdf, particularly at the 'tail' regions.

Before addressing possible remedies for the same, we summarize the results of this section by saying that exact pdfs can be computed using the PF operator based approach and the computations are shown to be much faster compared to a MC simulation aiming to obtain an approximating histogram distribution of similar smoothness. One can also get the most probable trajectories as shown in Fig. 3 and 4, by tracing the locus of the modes of the marginal pdfs. Fig. 5 shows the evolution of the corresponding 3σ confidence ellipsoid.

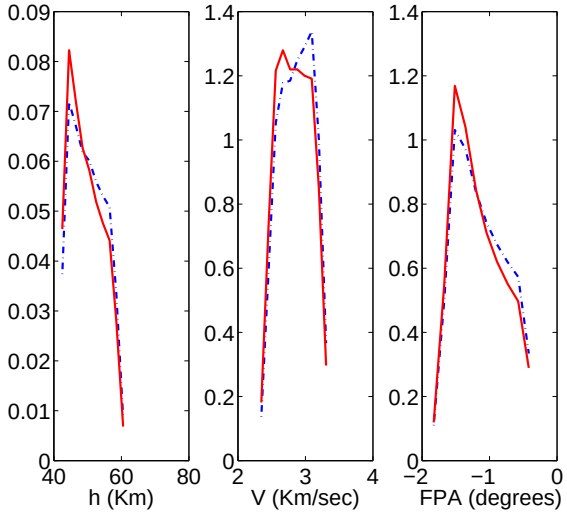

(a) MC (blue, dotted) and PF (red, solid) marginals with dpd = 10

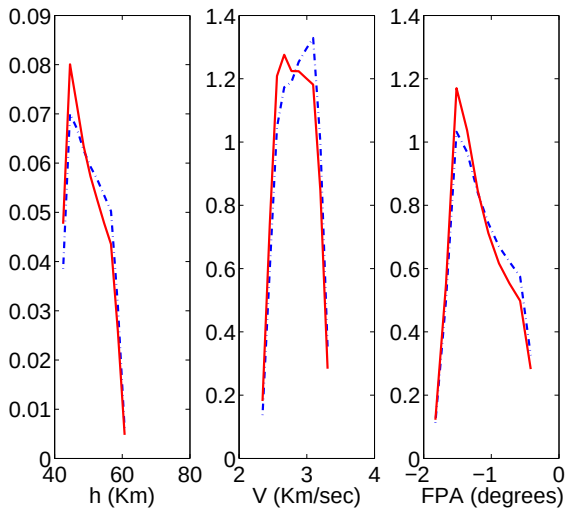

(b) MC (blue, dotted) and PF (red, solid) marginals with dpd = 20

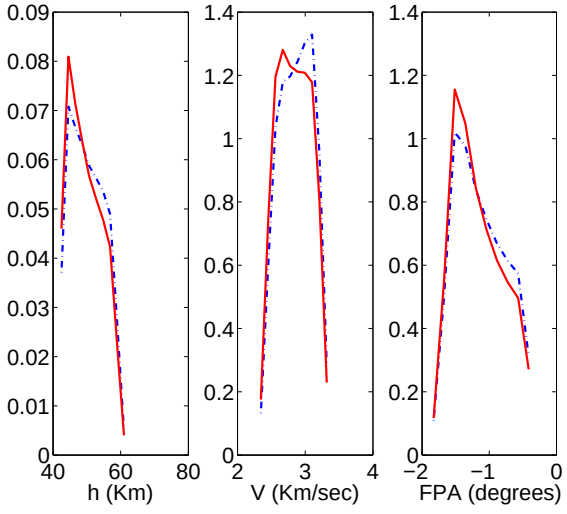

(c) MC (blue, dotted) and PF (red, solid) marginals with dpd = 30

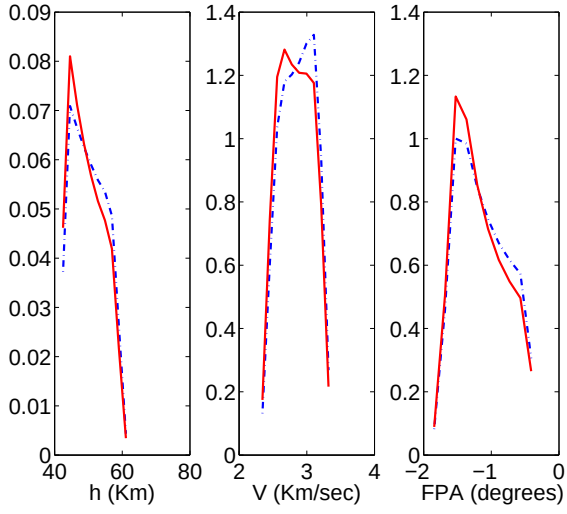

(d) MC (blue, dotted) and PF (red, solid) marginals with dpd = 40

Figure 1. Snapshots of marginal pdfs at 267^{th} second for the three state model with only intial condition uncertainties.

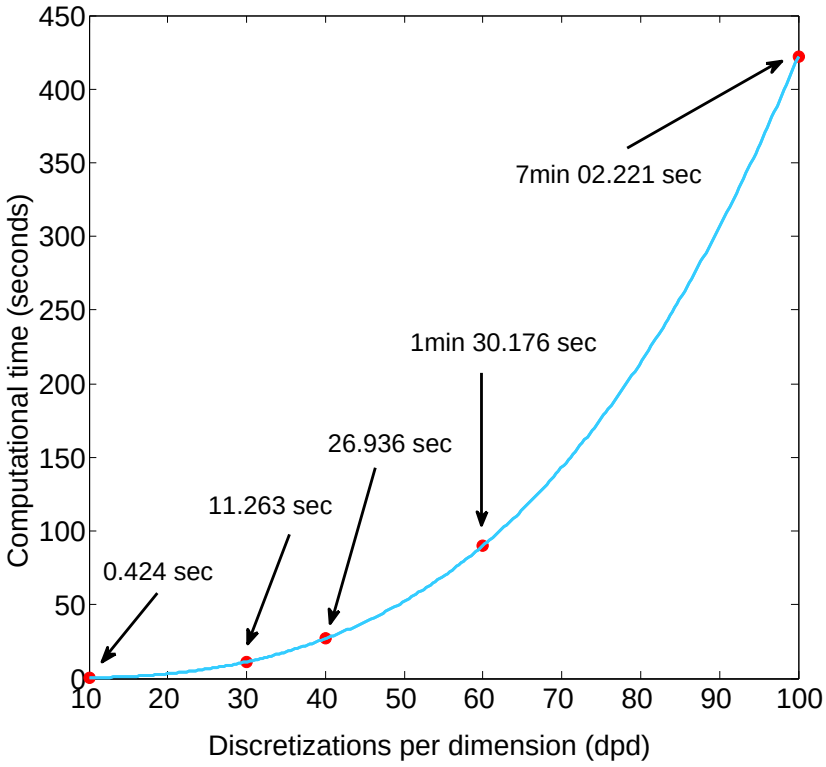

Figure 2. Better histogram approximations of the pdfs need MC simulations with more dpd. However, CPU time needed to perform MC simulation grows exponentially with the increase in dpd while the pdfs shown in Fig. 1(b) can be computed in 0.522 seconds.

V. Improving computational performance

In the last section, we have seen that the transfer operator based method, in general, yields exact pdf with significant computational savings compared to the large-scale brute-force MC simulations resulting crude approximation(s) of the pdf(s). However, Table 1 revealed two potent issues, particularly for systems with many uncertain states and parameters.

1. Since the initial uncertainties were transcripted through a grid, the number of gridpoints (in the extended state space) blows up exponentially resulting in huge size of the output files. Filesize of several giga-bytes containing scattered data becomes virtually impossible for further post-processing.

2. Also, the computational time becomes very large when we deal with higher dimensional systems.

The crux of both the problems is that the samples of the initial joint pdf lie on a grid. If somehow, we can sample the initial joint pdf without creating a grid, then we can expect improvements on both the aspects mentioned above. Since we are considering uniform initial distribution in this paper, we will discuss a methodology to sample any user-specified number of samples in any desired dimension and show how that can enhance the performance. For the more general case of any given joint pdf, one can do the same using Markov Chain Monte Carlo[15–17] (MCMC) method.

In our case for generating samples of uniform joint pdf, a pseudo-random number generator was utilized to generate low discrepancy sequences.[18] The same reference contains detailed treatment about the theoretical aspects of this procedure. A very brief outline is provided in the Appendix. We implemented Halton sequence for generating pseudo-random numbers in any specified dimensional hypercube and then scaled the data to exhibit 5% uniform uncertainties about respective nominals. The major advantage is that now we can specify the number of intial samples to be generated in any given dimension, thereby vastly reducing the number of samples which would otherwise be impossible in a gridded world. These initial samples were then taken

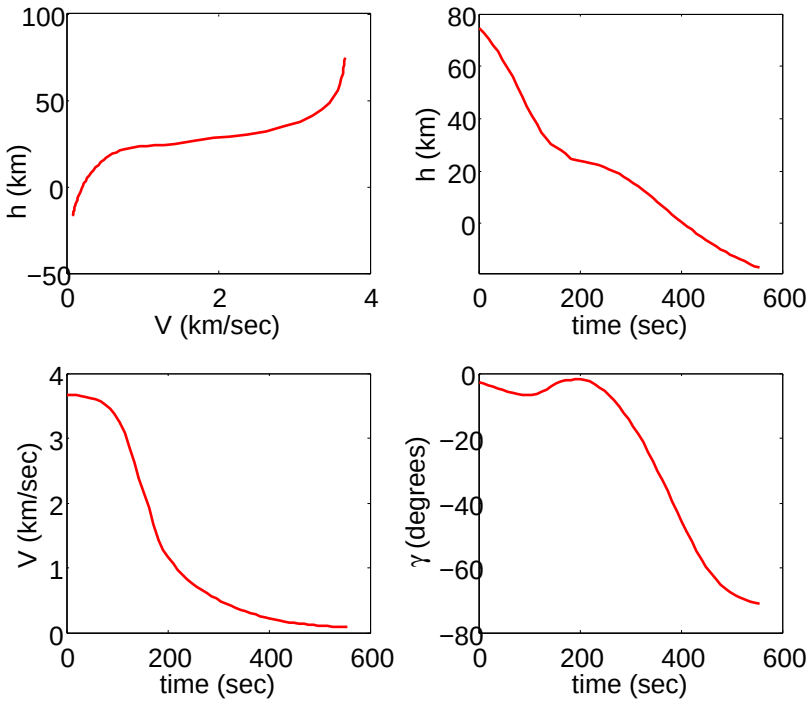

Figure 3. Most probable trajectory obtained by tracing the locus of the modes of the marginal pdfs obtained through PF operator approach with dpd = 10.

as input to the PF operator based method to evolve the pdf. The file size and computational time were drastically reduced. Furthermore, since the Halton sequences were generated through purely deterministic algorithm, the creation of samples is much faster than other alternatives.

3 test cases were run to test the efficacy of this method, all with 2000 Halton points. First, the three state model with both state and parametric uncertainties, the six state model with only state uncertainties and the same with both state and parametric uncertainties. A comparative assesment can be made about the computational savings by looking at Fig. 6 which shows how the file size grows for different test cases with different simulation methods. The drastic reduction in filesize in Fig. 6(c) is accompanied by the fact that the computational times for the three bars are 0.981 seconds, 1.521 seconds and 2.170 seconds respectively. The computational times for the MC method and for the PF method with grid were listed in Table 1.

VI. Conclusion

A computational framework is provided in this paper to methodically evolve the state and parametric uncertainties in the form of a joint pdf with numerical efficiency rather than attempting hugely expensive brute-force MC simulations. It is shown that the framework can handle mission critical planetary EDL simulations which typically feature uncertainty in large number of states and parameters. A comparison has been made between the proposed approach and the MC method for high-dimensional nonlinear dynamical systems like hypersonic entry in Mars atmosphere. Moreover, it's emphasized that by suitably choosing meshless intial samples, one can execute the proposed method with significant computational savings.

The authors are presently working towards building a robust and fast post-processing framework which can more efficiently handle high-dimensional scattered data for applications such as risk analysis.

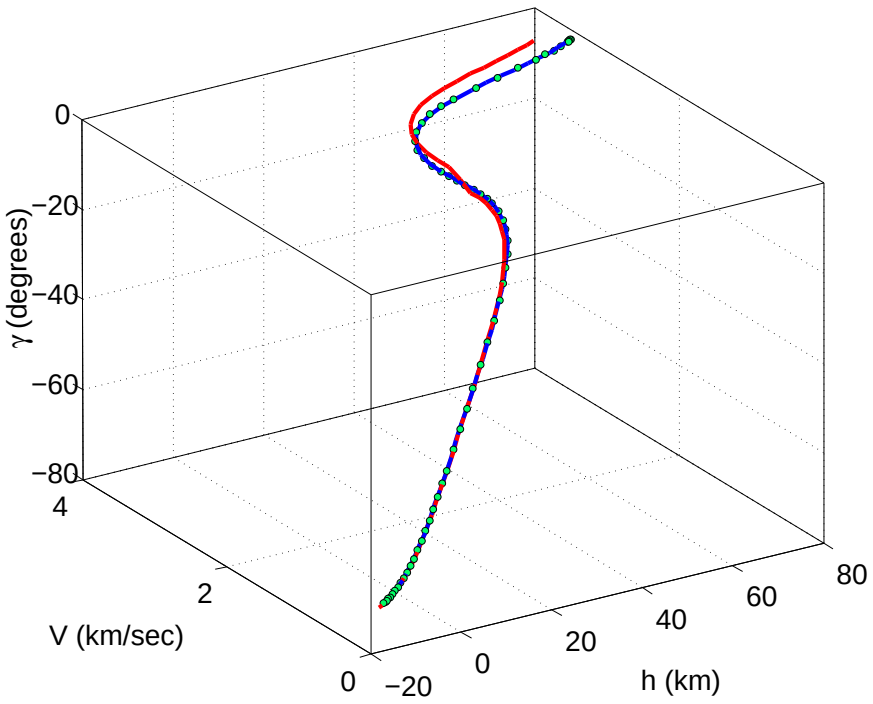

Figure 4. A comparison of the mean (blue solid line) trajectory, nominal trajectory (green circles) and most probable trajectory (red solid line). The deviation between the mean and most probable trajectories reinstate the importance of propagating the full pdf instead of evolving the moments as in parametric methods.

Appendix

A. An outline of Halton sequence generation and its application for intial pdf sampling

The basic idea behind generating the initial joint pdf samples through pseudo-random number generators is to break the 'curse of dimensionality' incurred due to gridding the extended state space. However, even then, the grid only exists at the initial instant as the state space deforms with time and the samples get scattered (e.g. Fig. 7). Hence one may find it worthy to generate samples of the initial pdf in a meshless fashion. Further, one must account that such sample generation algorithm must be fast enough to provide practical advantages. Halton sequence is suitable in these respects as it generates vector of such samples in unit interval. Cartesian product of that sequence yields multidimensional scattered data, most importantly all through a deterministic algorithm.

In 1D case, a prime number (say 2) is taken and the sequence of natural numbers are written with respect to that base and then they are mapped to the unit interval. This is known as *Van der Corput sequence*. So the steps are

1. Write a sequence of natural numbers with respect to a prime base (say 2).
2. Map the resulting number to the unit interval (e.g. for base 2, reverse the order of digits of the binary number and determine the decimal number corresponding to that reversed binary number.)

For *Halton sequence*, the above is done for each dimension with different prime bases (2, 3, 5 etc.). While dealing with high dimensions, one must make sure to generate enough prime numbers to be used as bases. Then the permutation of these vectors result multidimensional scattered data. At the end, one must scale the generated data from the unit hypercube to the domain of interest. Fig.8 shows 2000 such Halton points in 3 dimensions.

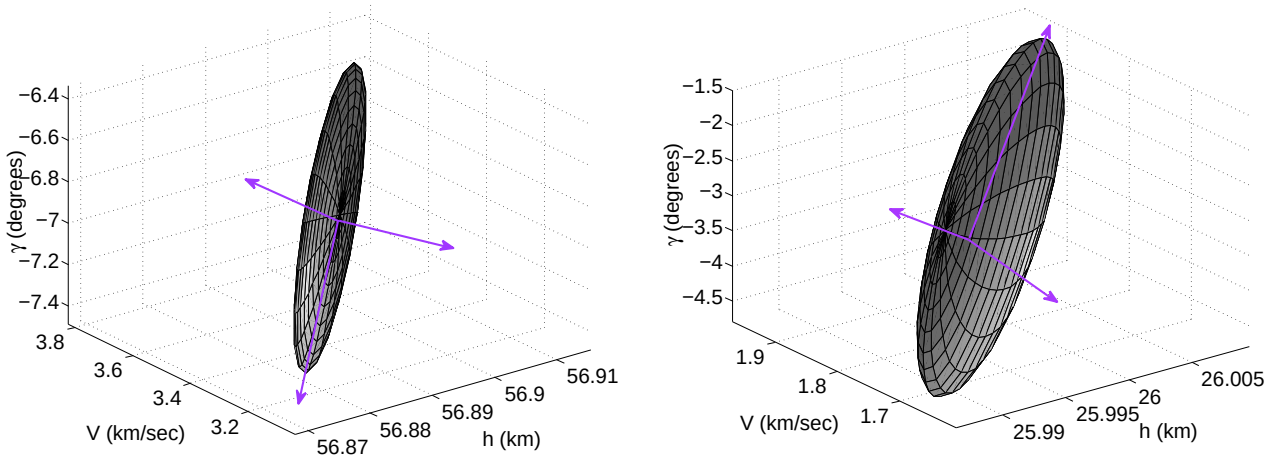

(a) Snapshot of the 3σ confidence ellipsoid after 10 time steps

(b) The same after 20 time steps

Figure 5. Evolution of the 3σ confidence ellipsoid for the three state model with only intial condition uncertainties, simulated with dpd = 10. The purple arrows show the instantaneous eigenvectors of the precision matrix (inverse of the covariance matrix), signifying directions of maximum and minimum variance.

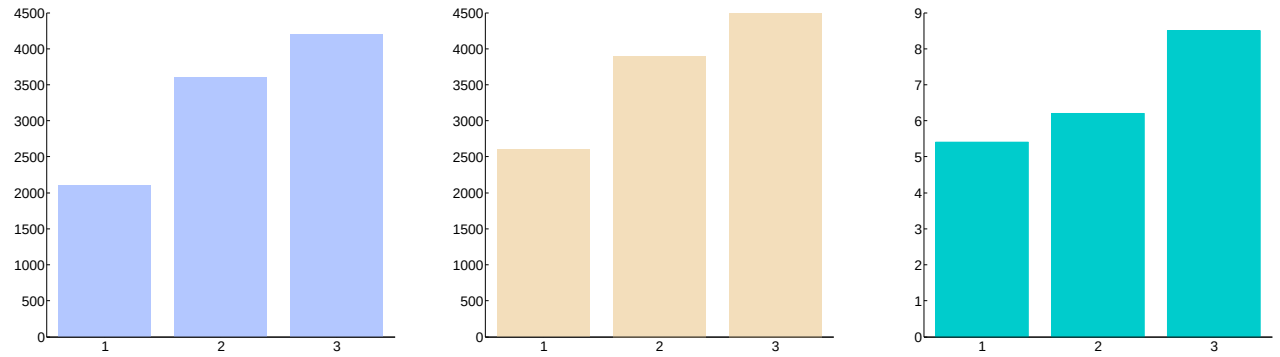

(a) MC simulations

(b) PF simulations with grid

(c) PF simulations with Halton points

Figure 6. Comparison of file size variation for different methods. The indices 1, 2 and 3 in the horizontal axes of each of the histograms correspond to the three state model with both state and parametric uncertainties, the six state model with only state uncertainties and the same with both state and parametric uncertainties, respectively. The vertical axes show filesize in MB.

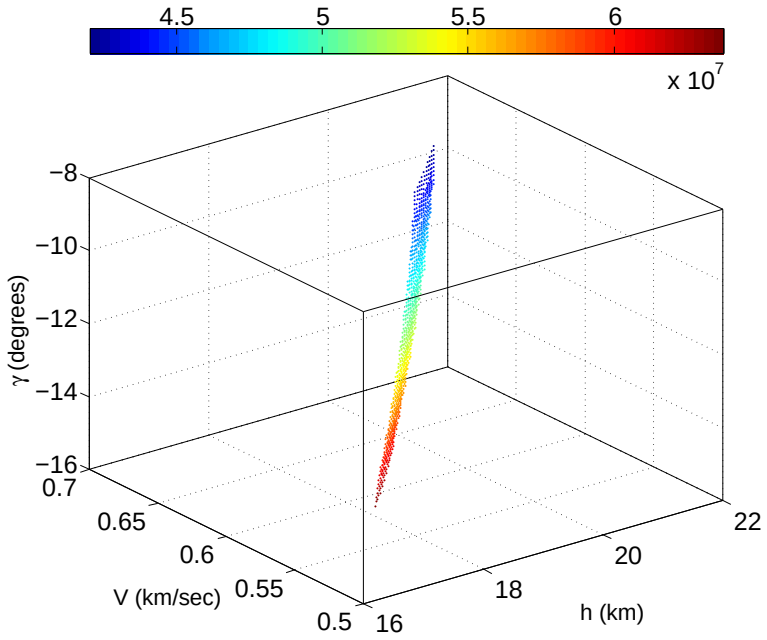

Figure 7. The deformed state space at 35^{th} non-dimensional time-step for the three state model with only initial condition uncertainties. The color is mapped proportional to the joint pdf value at the data-site.

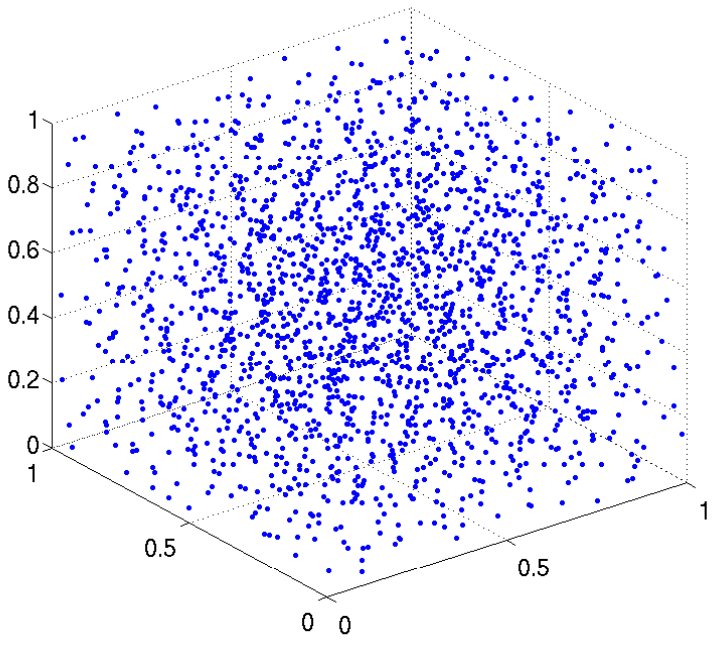

Figure 8. 2000 pseudo-random Halton points in the unit cube.

Acknowledgments

This research work was supported by NASA Jet Propulsion Laboratory (JPL) Director's Research and Development Fund DRDF-FY09 with J. (Bob) Balaram (section 347) as JPL principal investigator and Aron Wolf (section 343) as JPL co-investigator.

References

[1]Spencer, D. A., and Braun, R. D., "Mars Pathfinder Atmospheric Entry: Trajectory Design and Dispersion Analysis", *Journal of Spacecrafts and Rockets*, Vol.33, No.5, 1996, pp. 670-676.

[2]Desai, P. N., Braun, R. D., Powell, R. W., Engelund, W. C., and Tartabini, P. V., "Six-Degree-of-Freedom Entry Dispersion Analysis for the METEOR Recovery Module", *Journal of Spacecrafts and Rockets*, Vol.34, No.3, 1997, pp. 334-340.

[3]Desai, P. N., Mitcheltree, R., and Cheatwood, F., "Entry Dispersion Analysis for the Stardust Comet Sample Return Capsule", *Journal of Spacecrafts and Rockets*, Vol.36, No.3, 1999, pp. 463-469.

[4]Braun, R. D., Mitcheltree, R., and Cheatwood, F., "Mars Microprobe Entry-to-Impact Analysis", *Journal of Spacecrafts and Rockets*, Vol.36, No.3, 1999, pp. 412-420.

[5]Striepe, S. A., Queen, E. M., Powell, R. W., Braun, R. D., Cheatwood, F., Aguirre, J. T., Sachi, L. A. and Lyons, D. T., "An Atmospheric Guidance Algorithm Testbed for the Mars Surveyor Program 2001 Orbiter and Lander", *AIAA Atmospheric Flight Mechanics Conference and Exhibit, Boston, MA*, 1998.

[6]Striepe, S. A., Way, D. W., Dwyer, A. M. and Balaram, J., "Mars Science Laboratory Simulations for Entry, Descent, and Landing", *Journal of Spacecrafts and Rockets*, Vol.43, No.2, 2006, pp. 311-323.

[7]Congdon, W. M., "Ablation Model Validation and Analytical Sensitivity Study for the Mars Pathfinder Heat Shield", 30^{th} *AIAA Thermophysics Conference, San Diego, CA*, 1995.

[8]Lasota, A., and Mackey, M. C., *Chaos, Fractals and Noise: Stochastic Aspects of Dynamics*, Applied Mathematical Sciences, Vol.97, Springer-Verlag, NY, 1994.

[9]Ehrendorfer, M., "The Liouville Equation and its Potential Usefulness for the Prediction of Forecast Skill. Part I: Theory", *Monthly Weather Review*, Vol.122, No.4, 1994, pp. 703-713.

[10]Vinh, N. X., Busemann, A., and Culp, R. D., *Hypersonic and Planetary Entry Flight Mechanics*, University of Michigan Press, Ann Arbor, 1980.

[11]Noton, M., *Spacecraft Navigation and Guidance*, Advances in Industrial Control, Springer-Verlag, NY, 1998.

[12]Mellodge, P., and Kachroo, P., "Uncertainty Propagation in Abstracted Systems", *Model Abstraction in Dynamical Systems: Applications to Mobile Robot Control*, Lecture Notes in Control and Information Sciences, Vol.379, Springer Berlin/Heidelberg, 2008, pp. 97-110.

[13]http://marsoweb.nas.nasa.gov/landingsites/msl/topsites/mawrth_vallis

[14]Golombeck, M., Grant, J., Vasavada, A., R., Grotzinger, J., Watkins, M., Kipp, D., Noe Dobrea, E., Griffes, J., and Parker, T., "Selection of Four Landing Sites for the Mars Science Laboratory", http://marsoweb.nas.nasa.gov/landingsites/msl2009/memoranda/MSL_Site_Selection_March2009.pdf, March, 2009.

[15]Andrieu, C., Frietas, N. D., Doucet, A., and Jordan, M. I., "An Introduction to MCMC for Machine Learning", *Machine Learning*, Vol.50, 2003, pp. 5-43.

[16]Gilks, W. R, Richardson, S., and Spiegelhalter, D., *Markov Chain Monte Carlo in Practice*, Interdisciplinary Statistics, Chapman & Hall/CRC Florida, 1996.

[17]Bishop, C. M, *Pattern Recognition and Machine Learning*, Information Science and Statistics, Springer NY, 2007.

[18]Niederreiter, H., *Random Number Generation and Quasi-Monte Carlo Methods*, CBMS-NSF Regional Conference Series in Applied Mathematics, Society for Industrial and Applied Mathematics Pennsylvania, 1992.